THE JOURNAL OF PHYSICAL CHEMISTRY B

ARTICLE

pubs.acs.org/JPCB

Photophysical, Electrochemical and Crystallographic Investigations of the Fluorophore 2,5-Bis(5-*tert*-butyl-benzoxazol-2-yl)thiophene

M. Amine Fourati, Thierry Maris, W. G. Skene,* C. Géraldine Bazuin,* and Robert E. Prud'homme*

Département de Chimie, Centre de recherche sur les matériaux auto-assemblés (CRMAA/CSACS), Université de Montréal, CP 6128, Succ. Centre-Ville, Montréal, Québec, Canada, H3C 3J7

Supporting Information

ABSTRACT: The photophysics of 2,5-bis(5-*tert*-butyl-benzoxazol-2-yl)thiophene (BBT) were investigated for assessing its limitations for use as a universal fluorophore and as a viable sensor for both polymeric and solution studies. This is of importance given the limitations of currently used materials. BBT's steady-state and time-resolved fluorescence were additionally investigated to correlate its solid-state features, observed by fluorescence spectroscopy when mixed in poly (1,4-butylene succinate) (PBS) films, with its single crystal characteristics. The conjugated fluorophore was found to be highly fluorescent, with absolute quantum yields of (Φ_{fl}) $\geq$ 0.60. The Φ_{fl} values were high, regardless of solvent polarity and proticity and whether alone or in polymeric films. The major competitive fluorescence quenching pathway was found to occur by intersystem crossing to the triplet state. This was confirmed by laser flash photolysis in which the BBT triplet absorbed at 500 nm. The triplet transient was confirmed by quenching studies with 1,3-cyclohexadiene. Meanwhile, nonradiative deactivation of BBT's singlet excited state by internal conversion was found to be negligible. In solution and especially when distributed in semicrystalline PBS, BBT exhibits spectral changes and a bathochromic shift as a function of concentration due to aggregation of ground state molecules, which is present even at low BBT concentrations. Consistent monoexponential lifetimes on the order of ~2 ns were observed regardless of solvent and independent of both the excitation wavelength and concentration. The constant excited state kinetics confirm the absence of a singlet excited state deactivation by excimer formation. The electrochemistry of BBT demonstrated that it is irreversibly oxidized and the resulting radical cation is unstable. Conversely, the cathodic process, resulting in the radical anion, is reversible, confirming its n-doping character. Crystallographic studies revealed that the planes described by the benzoxazolyl moieties are twisted from the plane described by the central thiophene. Several weak C−H···π and π−π intermolecular interactions were also observed. BBT's high solubility in common solvents combined with its measured enhanced optoelectronic properties make it a candidate as a universal fluorophore reference and smart material for both polymeric and solution studies.

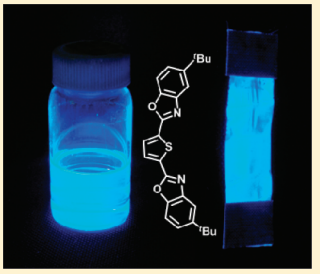

1. INTRODUCTION

4,4′-Bis(2-benzoxazolyl)stilbene (BBS) has interesting optical properties that have led to its use as photoactive switches[1,2] and as an optical brightener for textiles[3] and in detergents and other materials.[4] These properties have also made it ideal for use in smart materials by probing temperature and deformation in polymer films,[5−7] upon formation or breaking of BBS excimers, respectively, leading to a color change under UV illumination. Despite these spectroscopic advantages, a major drawback of BBS is its limited solubility in only high-boiling chlorinated solvents, specifically hot tetrachloroethane. Moreover, such solvents are both toxic and expensive, which restricts the usefulness of BBS. The stillbenoid structure of the latter further provides an efficient fluorescence quenching mode possible by *E*−*Z* photoisomerization.[8] This excited state quenching process results in low fluorescence quantum yields in solution and further limits the usefulness of BBS in certain fields. Therefore, a fluorophore exhibiting solubility in a broad range of solvents with consistent high fluorescence yields that does not suffer from the limitations of BBS is required.

In contrast to BBS, 2,5-bis(5-*tert*-butyl-benzoxazol-2-yl)thiophene (BBT) is soluble in a wide range of organic solvents. Moreover, BBT cannot photoisomerize, which can increase the chances for an intrinsic fluorescence in solution. It also absorbs and emits in the visible owing to its extended π-conjugation. As a result of its collective optical properties that can be visibly tracked by the naked eye concomitant to its solubility in a broad range of process compatible solvents, BBT has found many optical applications. These include the use as an optical brightener,[9] and as a whitening agent in many polymers and textiles,[10] in addition to uses in various optoelectronic applications.[11−21] BBT further shows excellent heat stability, and it can be used to improve the color of various plastics.

The similar optical properties of BBT and BBS, but the much wider solubility range of BBT, combined with its inherent fluorescence, make BBT a potential replacement of BBS. Yet, despite BBT's use in various applications because of its spectroscopic and thermal properties, no extended optoelectrochemical studies have been undertaken. In particular, it would be beneficial

Received: May 28, 2011
Revised: September 14, 2011
Published: September 14, 2011

Chart 1. Structures of 2,5-Bis(5-*tert*-butyl-benzoxazol-2-yl)thiophene (BBT) and 4,4′-Bis(2-benzoxazolyl)stilbene (BBS)

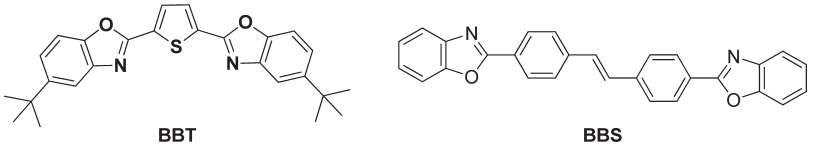

to probe the photophysics of BBT and examine its solvent dependent fluorescence. Such studies are pivotal for determining the fluorescence limitations of BBT and for its use as a universal fluorophore. Here, we report the optoelectrochemical and extensive photophysical properties of BBT, including its crystallographic data. Our purpose is to study in depth the BBT characteristics to correlate its solid-state properties, observed by fluorescence spectroscopy when mixed in poly(1,4-butylene succinate) (PBS) films, with its single crystal features. These features motivate a characterization as well as an investigation of the BBT photophysical properties to study the possibility of using BBT as a potential substitute of BBS.

EXPERIMENTAL SECTION

Materials. 4,4′-Bis(2-benzoxazolyl)stilbene (97%, melting point >300 °C) and 2,5-bis(5-*tert*-butyl-benzoxazol-2-yl)thiophene (99%, melting point ∼200 °C) were purchased from Aldrich Chemicals and used without further purification.

Poly(1,4-butylene succinate) (PBS) (Bionolle 1001) was graciously supplied by Showa Highpolymer Company (Japan). PBS is a semicrystalline polymer used primarily for the manufacturing of films and packaging and is degradable in compost or activated sludge. It is characterized by a glass transition temperature of −34 °C and a melting temperature of 113 °C.

Film Preparation. PBS-BBT films were prepared by melt-processing in a DDRV501/DIGI-SYS Plasti-Corder Brabender mixer by mixing ∼20 g of PBS and 0.02 to 2 wt % of BBT at 200 °C, at 50 rpm, for 10 min. The obtained material was compressed and molded between two aluminum foils in a Carver Laboratory Press at 200 °C, under a pressure of 5 tons. The samples were then introduced in a cold press and were left to cool slowly to room temperature before removal from the press, under a pressure of 2 tons. Films with thicknesses of 60−120 μm were obtained.

Spectroscopic Measurements. Absorption measurements were done on a Varian Cary-500 UV−visible spectrometer, and the solvent absorption spectra were subtracted from the spectra of the analyzed samples. Fluorescence emission spectra were recorded at ambient temperature in 10 mm cuvettes exciting at the corresponding absorption maximum with an Edinburgh Instruments FLS-920 combined steady-state and time-resolved fluorometer. Both the front-face and 90° geometries were used for solution fluorescence studies. Meanwhile, the front-face geometry was exclusively used for both polymeric films and powder (prepared by using a press for KBr pellets to get compacted pastilles). The fluorescence lifetimes were measured according to standard time-correlated single photon counting (TCSPC) methods with the FLS-920 by fitting with a mono-exponential decay function. The calculated values have an experimental error of ∼10%. Fluorescence quantum yields were used to quantify the efficiency of the emission process by taking the ratio of photons absorbed to photons emitted through fluorescence at a particular wavelength in the same period of time. Absolute fluorescence quantum yields were measured

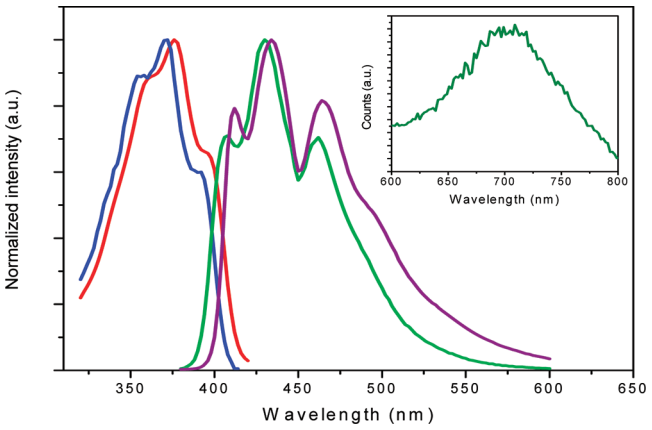

Figure 1. Normalized BBT and BBS absorption and emission spectra in tetrachloroethane: blue, BBT absorption; red, BBS absorption; green, BBT emission; purple, BBS emission. Inset: BBT phosphorescence emission in a 4:1 ethanol/methanol matrix at 77 K.

using an integrating sphere that was calibrated with basic ethanolic fluorescein. These were done by integrating over the entire emission spectrum from baseline to baseline, as previously reported.[22] Phosphorescence emission spectra were recorded at 77 K in a solid matrix of 4:1 ethanol/methanol using a Cary Eclipse phosphorescence spectrophotometer.

Peak decomposition was carried out with the Origin Pro8 software by increasing gradually the number of peaks until obtaining a peak sum similar to the studied spectrum. HOMO and LUMO molecular orbitals were calculated semiempirically using DFT methods available in Spartan 06 with the 6-31g* basis set. The bond angles, distances, torsions, and other parameters used for the theoretical calculations were experimentally derived from the X-ray data for BBT.

Laser Flash Photolysis (LFP). The triplet−triplet absorption spectra were measured in anhydrous acetonitrile using a Luzchem mini-LFP system, excited at 355 nm from the third harmonic of a Continuum YAG:Nd Sure-lite laser using a 175 W xenon lamp. An average of 15 shots per wavelength was used for generating the transient absorption spectrum. The samples were dissolved in anhydrous acetonitrile in static quartz cuvettes and assured to have an absorbance of <0.4. All samples were purged with nitrogen for at least 20 min before LFP analyses.

Crystallographic Study. BBT light green plate crystals suitable for X-ray diffraction analysis were obtained by slow evaporation from a saturated 1,2-dichlorobenzene solution. The single crystal study was carried out by using a Bruker Microstar diffractometer with a rotating anode generator producing Cu K_α radiation, a kappa goniometer and a CCD platinum 135 detector.

H atoms were positioned geometrically and refined with a riding model, with C−H distances of 0.95 Å and Uiso (H) values constrained to be 1.2 times Ueq of the carrier atom.

dx.doi.org/10.1021/jp207136k |J. Phys. Chem. B 2011, 115, 12362–12369

Table 1. BBT Spectroscopic Data Measured in Different Solvents at $\lambda_{exc} = \lambda_{ab}$

	ε_{max} [a] (M^{-1} cm^{-1})	λ_{ab} [b] (nm)	λ_{fl} [c] (nm)	φ_{fl} [d]			
[BBT] (mM)				0.002	0.02	0.2	2
1,2-Dichlorobenzene	33000	379	437			0.96	0.93
Acetonitrile	20000	371	432	0.76	0.74	0.73	
Butanol	42000	375	434	1	0.87	0.83	0.83
Ethanol	35000	373	434	1	0.82	0.78	
EtOH/MeOH 4:1	26000	373	434		0.75	0.77	
Methyl cyclohexane	37000	373	426	0.66	0.66	0.58	0.54
DMF	35000	374	434	0.87	0.83	0.82	0.80
Cyclohexane	52000	372	426	0.80		0.68	
Benzene	27000	377	434	0.82	0.84	0.80	0.75
Toluene	38000	376	434	1	0.93	0.87	0.81
Tetrachloroethane	31000	378	440	1	0.97	0.91	0.88
THF	35000	374	432	0.78	0.77	0.75	0.68

[a] Molar absorptivity. [b] Maximum absorption. [c] Maximum fluorescence. [d] Absolute quantum yields were calculated with an integrating sphere.

RESULTS AND DISCUSSION

Absorbance and Emission Studies. Solution absorbance studies of both BBS and BBT were first performed to determine the appropriate excitation wavelength for fluorescence studies. According to Figure 1, both well-known fluorophores, BBS and BBT, are characterized by virtually identical features. Indeed, the absorption spectra exhibit three well-defined peaks at 354, 372, and 392 nm for BBS and at 358, 378, and 398 nm for BBT. The emission spectra also show three well-defined vibronic peaks located at 412, 434, and 464 nm for BBS and at 408, 430, and 462 nm for BBT. It can be seen that the fluorescence spectra are a symmetric image of the absorption spectra (Kasha's law).[23] It should be noted that there was no distinct change in absorption peaks for both compounds in tetrachloroethane with increasing concentration. Moreover, both fluorophores are highly conjugated and exhibit a high fluorescence. The BBS dye is visually yellow, whereas BBT is green, which enables its use as a color indicator. This comparison between BBS and BBT, showing their similarity, indicates that it might be possible, from a spectroscopic point of view, to replace BBS with BBT. An advantage of BBT is its high solubility in standard organic solvents, in constrast to BBS, which is only sparingly soluble in hot tetrachloroethane and other high-boiling chlorinated solvents.

Fluorescence Investigation. To study the BBT characteristics in comparison with BBS, its photophysical properties were measured in a series of 12 solvents of varying polarity for investigating their effect on the BBT ground and excited states. Slight bathochromic shifts have been observed in all solvents, with a shift in absorbance of 8 nm between acetonitrile and 1,2-dichlorobenzene and a shift in fluorescence of 14 nm upon increasing polarity from cyclohexane to tetrachloroethane (Table 1). A rough estimate of the energy gap (E_g = 3.1 eV) is derived from the onset of the absorption in the red region of the spectrum. The absolute energy difference between the ground (HOMO) and excited (LUMO) states can be calculated from the intercept of the normalized absorption and emission spectra. According to the spectroscopically measured values, the energy gaps are unaffected by the solvent polarity and concentration. Quantum yields on the order of 0.6−0.7 were measured for BBT concentrations ranging up to 6 wt % in PBS films. The fluorescence yield was found to be invariable with either freshly prepared PBS-BBT-2 wt % films or films stretched to a local strain of either 190 or 230%. The consistent emission yields for relaxed and stretched films imply the absence of any molecular rearrangement induced by the polymer deformation. This is probably due to the banana shape of the BBT molecule, encouraged by the 2,5-disubstitution of the central thiophene aromatic ring, and mainly the terminal *t*-butyl groups, which weaken the $\pi-\pi$ intermolecular interactions and avoid the formation of BBT excimers. Unlike BBT, BBS neighboring molecules can easily form $\pi-\pi$ and C−H···π intermolecular interactions[24] that facilitate the formation of BBS excimers and, thus, their use as molecular probes in polymeric smart materials, based on a color change that remains unfortunately absent for BBT even by increasing the fluorophore concentration.

Quantum yield measurements are usually done by relative actinometry. An actinometer is a chemical system that undergoes a light-induced reaction at a certain wavelength for which the quantum yield is accurately known.[25] The limitation of this method is that the reference must both absorb and emit within the same wavelength as the compound to be measured, in addition to having approximately the same emission yield. Moreover, the absolute quantum yield of the reference must be accurately known for a given solvent. The cumulative experimental errors for relative actinometry lead to quantum yields that can be known to within 80% accuracy at best.[26] Absolute and accurate quantum yields can, however, be obtained with an integrating sphere.[27] Given that previously reported BBT emission yields were done by relative actinometry in a limited number of solvents, we measured its absolute quantum yields in twelve different solvents.

It is evident from Table 1 that BBT fluoresces strongly and is independent of solvent polarity and proticity, which may allow its use as a suitable replacement for conventional fluorophores such as BBS. Moreover, BBT's thermal stability, which excludes complications due to dark reactions; its direct spectrophotometric analysis as well as its commercial availability;[25] and its high fluorescence quantum yields, whatever its state, make it a suitable reference for actinometric fluorescence studies. These collective properties make BBT an attractive universal fluorophore and sensor probe. For solutions having a quantum yield of 1, deactivation occurs only by fluorescence, but the measured quantum yields are less than unity in most solvents, implying the presence of deactivation modes other than fluorescence. Additional spectroscopic modes were subsequently investigated to assign the competing fluorescence

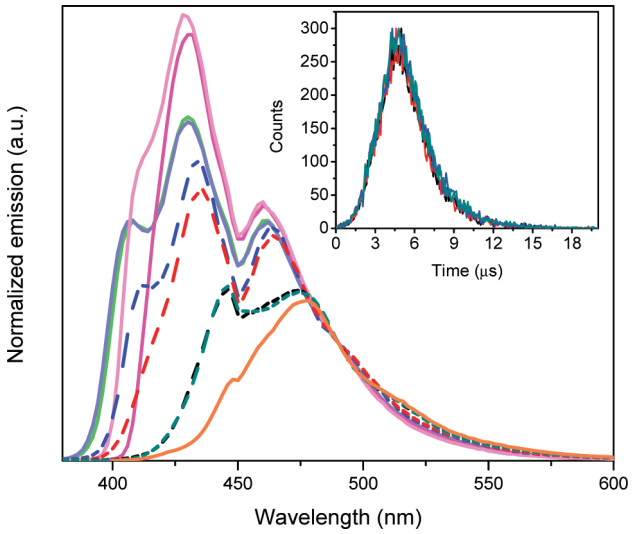

Figure 2. Normalized BBT fluorescence spectra at various BBT concentrations in THF (light green, 2 μM; blue-purple, 0.02 mM; magenta, 0.2 mM; light pink, 2 mM), when dispersed in polybutylene succinate films (blue, 0.02 wt %; red, 0.2 wt %; black, 2 wt %; dark cyan, 6 wt %) and as a powder (orange). Inset: BBT fluorescence kinetics monitored at 412 (black line), 432 (red line). 460 (blue line), and 500 nm (green line) in THF at ambient temperature at a concentration of 0.15 mM taking into account the IRF.

deactivation modes and for ensuring that these would not eventually suppress the desired fluorescence under specific conditions.

Temperature-dependent fluorescent studies were subsequently undertaken to assign the competing excited state deactivation processes responsible for the observed fluorescence below unity (vide supra). At 77 K, deactivation modes by bond rotations are normally suppressed, and internal conversion (IC) deactivation can therefore be calculated at this temperature according to $\Phi_{IC} \approx \Phi_{fl}$ (77 K) $- \Phi_{fl}$ (RT). We observed that the fluorescence quantum yield increased by 9%, from 0.75 to 0.82 in an ethanol/methanol matrix at 77 K relative to that at room temperature. The observed increase confirms that deactivation by IC occurs, albeit only a minor energy dissipation pathway, probably via the thiophene−oxazole bond.

Solution, Solid-State, and Powder Fluorescence. The photophysical properties of BBT led us to study its optical and fluorescent properties in solution and in a polymer matrix, i.e., in poly(1,4-butylene succinate) (PBS). Like many other polymers, PBS is processed at temperatures well below the degradation temperature of BBT (>300 °C). Figure 2 shows the fluorescence spectra of BBT at various concentrations in THF, or when incorporated into PBS as well as a powder. The fluorescence spectra of the lowest BBT concentration, in solution (2 μM) or into PBS (0.02 wt %), are characteristic of a well-defined vibronic structure, attributed to radiative transitions 0−0, 0−1, and 0−2 for BBT monomers. Intensity changes occur upon increasing the BBT concentration, since the first vibronic peak decreases considerably to become a shoulder and further disappears upon increasing the BBT concentration from 2×10^{-3} to 2 mM in THF or from 0.02 to 0.2 wt % or higher in PBS. A bathochromic shift also occurs for both the second, from 429 (at 0.02 wt %) to 448 nm (at 6 wt %), and third peaks, from 461 (at 0.02 wt %) to 476 nm (at 6 wt %), by increasing the BBT concentration (Figure 4) while the first peak, after shifting from 406 to 412 nm, can no longer be followed. These two peaks are representative of relatively weak interactions when compared with the first peak. These emission spectral changes were observed whatever the proticity or polarity of the solvent (tested in all of the solvents listed in Table 1) and regardless of the state (solution or solid). Therefore, the change in the intensity of the lowest-wavelength peak at 462 nm is not a consequence of solvent−solute interactions, as is frequently observed in protic solvents. Moreover, since the absorption spectrum remains unchanged, even at high BBT concentrations, the disappearance of the high energy vibronic peak at 407 nm is not due to intermolecular interactions.

BBT has been widely used as an electron-transporting material interacting with a hole-transporting host material, such as poly(*N*-vinyl carbazole) and *N*,*N*′-diphenyl-*N*,*N*′-bis(3-methylphenyl)-[1,1′-biphenyl]-4,4′-diamine.[13,18,19] This results in a transient donor−acceptor complex between the excited state of the donor (BBT) and the ground state of the acceptor.[28] The broad emission peak at ∼500 nm might at first sight be attributed to such a transient complex. Both concentration-dependent emission and bimolecular lifetimes are expected for such a BBT eximer. However, the emission at 500 nm is present even at low concentrations, and it has a unimolecular lifetime. The measured lifetime of 1.7 ns is further comparable to that reported previously,[29] specific to BBT monomers. Interestingly, the measured unimolecular lifetime was also independent of the excitation wavelength and concentration (see Supporting Information). The lifetime of each vibronic peak was also identical and independent of concentration (inset Figure 2).

To ensure that the observed concentration dependent spectral trend was not a result of an artifact or from inner filter effects, the emission measurements in solution were additionally done using the front-face geometry. These undesired effects are significantly reduced with this geometry.[30] Consistent fluorescence between both the right-angle and front-face (see Supporting Information) excitation−emission geometries were observed and confirm that the concentration-dependent emission shifts are true effects. This was further corroborated with consistent bathochromic fluorescence shifts observed in both thin film and solid state that were also measured with the front-face geometry. Although the emission spectra were found to be independent of excitation wavelength, the excitation spectra were similar to the absorbance spectra. This suggests that the measured spectroscopic properties are those of the fluorophore and not from an artifact.

High quantum yields were also observed, regardless of concentration. These were calculated using an integrating sphere and by integrating over the entire range of the emission wavelengths relative to the scattering of the pure solvent.[22] The concentration-dependent spectral changes are similar to those observed for interchain π-stacking of conjugated polymers in thin films.[16,31] Although the concentration-dependent emission shifts of BBT are real, an inner filter effect cannot be entirely dismissed. This is in part because of the unknown effect of light scattering from BBT aggregates in PBS films. The collective spectroscopic data nonetheless suggest that the observed concentration-dependent spectral changes result from intermolecular interactions.

To better understand the concentration dependent fluorescence, the PBS-BBT-0.02 wt % emission spectrum was decomposed, and the relative distribution of the different peaks was calculated. As seen in Figure 3, the emission spectrum can be decomposed into four discrete peaks. The three high-energy peaks are assigned to BBT monomers, whereas the lower energy one is ascribed to BBT aggregates; the aggregate band was found

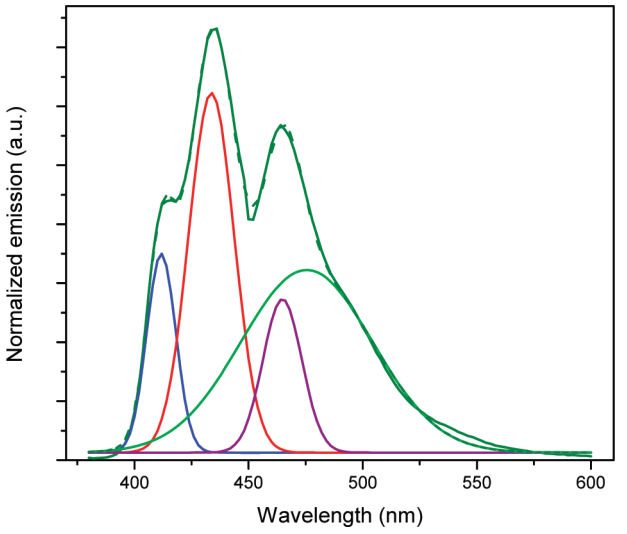

Figure 3. Multipeak fitting of the fluorescence spectrum of PBS-BBT-0.02 wt %: olive, emission; blue, peak 1; red, peak 2; purple, peak 3; green, peak 4 ; - - -, peak sum.

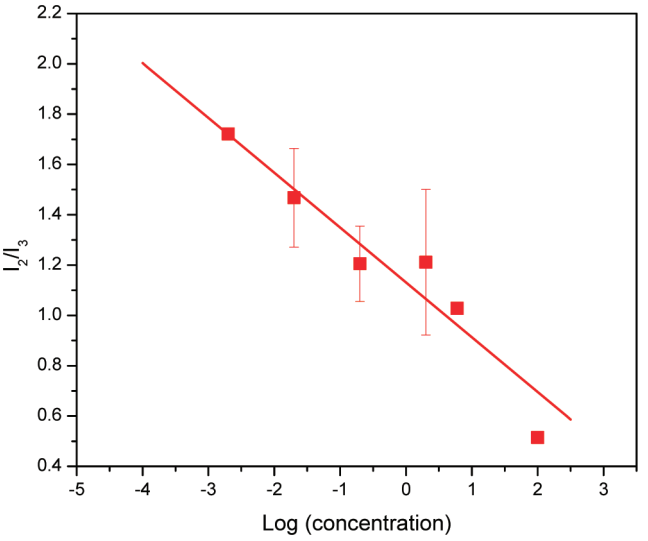

Figure 4. I_2/I_3 ratio as a function of BBT concentration in both PBS film and THF.

in the powder, in solution, and in polymeric samples, whatever the BBT concentration. From its relative area, it is found that the aggregate component is small at the lowest concentration but increases by increasing the BBT concentration, suggesting that the number of molecules influencing each other increases, involving a widening of this band to become a continuum. Indeed, the aggregate band is a consequence of the proximity of the orbitals of the different molecules inducing a splitting of the HOMO and LUMO energy levels.[32]

A similar emission at 516 nm is observed in the powder fluorescence spectrum and is attributed to BBT aggregates from the stacking of neighboring molecules (vide infra). In addition, the red-shifted spectrum of the powder, compared with the solution spectra, exhibits a shoulder at 448 nm and a well-defined peak at 478 nm, both belonging to the BBT monomers. BBT therefore exhibits both concentration and solution/PBS spectral shifts, confirming that it has local concentration probelike properties. No distinct concentration quenching has been observed within the concentration range in the polymeric state, confirming that PBS is an excellent host material to hold dye molecules such as BBT. On the other side, it is noteworthy that BBT is more easily dispersed in solution than in PBS, where the molecules are forced to come into contact with each other due to the PBS high crystallinity. Therefore, the emission spectra from low concentration solutions and films are very similar, as the aggregation is minimized. When the BBT concentration increases, there is a more pronounced bathochromic shift in solid-state films than in solution. This is essentially due to the increase of the $\pi-\pi$ intermolecular interactions in polymeric films, while the molecular rotations and vibrations, which are constrained in the solid-state, slow down the relaxations and broaden the energy band.

Figure 4 shows the I_2/I_3 ratio as a function of BBT concentration that is based on the average of three measurements. I_2/I_3 is the ratio of the intensity of the second and third fluorescence peaks, corresponding to the second and third vibronic transitions in the emission spectrum. Since the I_2/I_3 ratio decreases logarithmically with increasing BBT concentration, it can qualitatively be used for determining the local BBT concentration and

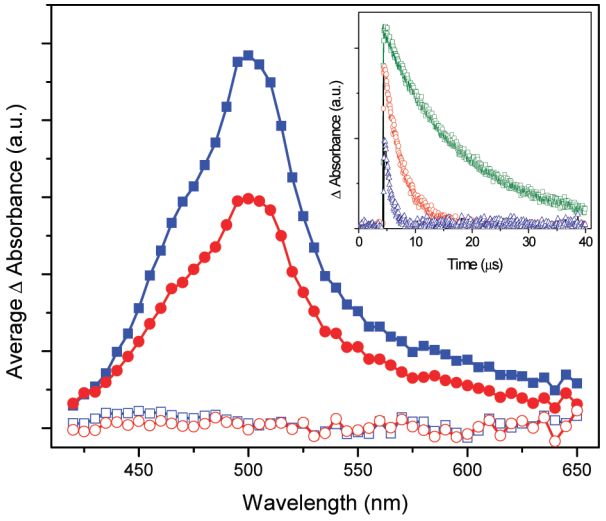

Figure 5. Transient absorption spectra of BBT recorded in acetonitrile at 5.9 and 9.8 μs before (blue solid square and red solid circle, respectively) and after (blue open box and red open circle, respectively) adding 60 μL of 1,3-cyclohexadiene (CHD) after a laser pulse at 355 nm. Inset: Decay kinetics of BBT monitored at 500 nm before (green) and after adding 20 (red) and 60 (blue) μL of 1,3-cyclohexadiene as a triplet state quencher.

its solubility, especially in polymeric films. The photophysical data demonstrate that spectral changes induced by concentration or intermolecular interactions can be detected even at low BBT concentrations, proving its high sensitivity as a potential local concentration probe.

Laser Flash Photolysis. Although high fluorescence quantum yields of BBT were measured in various solvents, the less than unity values imply additional excited state deactivation modes other than fluorescence. Laser flash photolysis was subsequently used to probe BBT's excited state and to identify long-lived transients. This is of particular interest given that its photophysical properties such as its time-resolved and steady-state behaviors have not been previously investigated. Figure 5 shows that

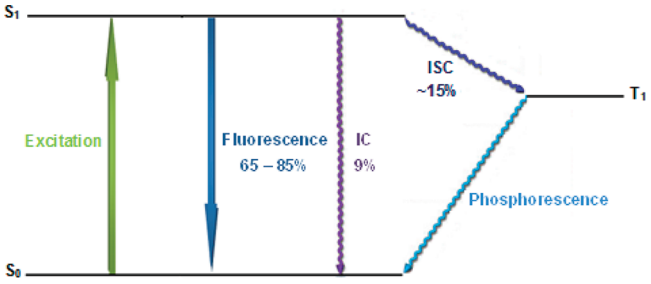

Figure 6. Schematic representation of the BBT energy dissipating processes.

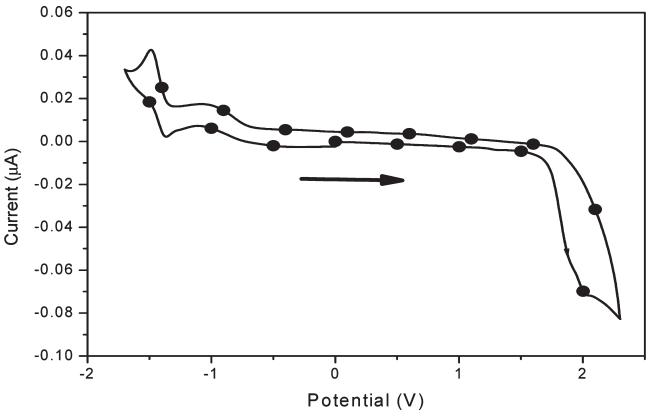

Figure 7. Cyclic voltammogram of BBT recorded in acetonitrile at 100 mV/s against Ag/AgCl with Bu_4NPF_6 as the supporting electrolyte.

direct excitation of BBT at 355 nm by laser flash photolysis produces a visible transient. To assign the strongly absorbing transient observed at 500 nm, it was quenched with successive additions of 1,3-cyclohexadiene (CHD). The transient intensity is then decreased while the lifetime is shortened with the addition of CHD, as shown in Figure 2 and its inset, respectively. It can be concluded that the observed transient is a triplet given that it is quenched with the known triplet quencher (CHD), taken together with its first-order kinetics (τ_0 = 14.4 μs). The triplet nature is further confirmed by the phosphorescence emission measured at 77 K (inset of Figure 1).

According to the energy conservation principle, that is, $\Phi_{fl} + \Phi_{IC} + \Phi_{ISC} \approx 1$, the singlet deactivation by intersystem crossing (ISC) to the triplet state can be approximated as contributing ~16% from the combined temperature-dependent fluorescence measurements. The observed triplet signal implies that BBT undergoes singlet deactivation by ISC. The collective steady-state and time-resolved measurements confirm that both nonradiative means, IC and ISC, are minor deactivation processes of the excited singlet manifold, relative to fluorescence. The simplified BBT Jablonski diagram for the deactivation processes and their estimated contributions are schematically depicted in Figure 6.

Cyclic Voltammetry. In addition to the photophysical properties of BBT, cyclic voltammetry was undertaken to probe the redox properties of BBT and to obtain important information relating to its stability at high temperatures. According to Figure 7, BBT undergoes a one-electron oxidation process, demonstrating its p-doping-type behavior. The high oxidation potential implies that BBT is stable under ambient conditions and that it is unexpected to be oxidized at high temperatures. The

Table 2. BBT Electrochemical Properties

E_{ox}[a] /V	E_{red}[b] /V	HOMO/eV	LUMO/eV	E_g[c]/eV
1.99	−1.40	6.28	3.23	3.1

[a] Oxidation potential. [b] Reduction potential. [c] Electrochemical energy-gap.

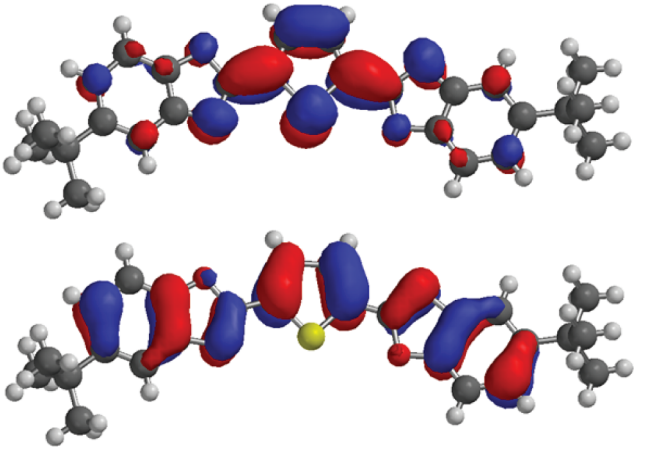

Figure 8. BBT LUMO (top) and HOMO (bottom) features calculated by DFT, using the 6-31g* basis set and the X-ray crystallographic data.

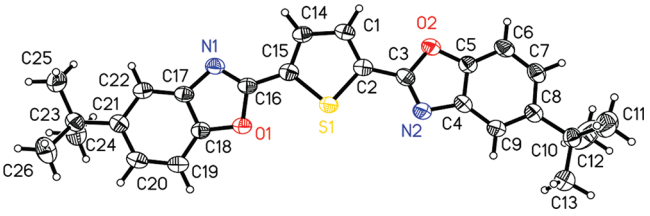

Figure 9. BBT molecular structure, with atomic displacement parameter ellipsoids at the 50% probability level.

electrochemical oxidation results in a highly reactive radical cation, confirmed by the irreversible behavior of cyclic voltammetry, regardless of the scan rate. Conversely, BBT is reversibly reduced at low potential, confirming its reversible n-doping character.

From the cyclic voltammetry data, the HOMO energy value can be calculated from the ionization potential (IP) according to IP = E^{ox}_{onset} + 4.4, where E^{ox}_{onset} is the oxidation potential onset in volts versus the SCE electrode. Similarly, the LUMO energy level is derived from the electron affinity (EA), calculated from the reduction onset potential (E^{red}_{onset}) according to EA = E^{red}_{onset} + 4.4. The HOMO and LUMO levels are reported in Table 2, which shows that the measured electrochemical E_g thus calculated is equal to the spectroscopic E_g. The electrochemical and spectroscopic data confirm that BBT is highly conjugated. This is further supported by the theoretically calculated molecular orbitals, using DFT, depicted in Figure 8. It is evident that the HOMO is delocalized across the entire molecule, responsible for BBT's high degree of conjugation. Conversely, the LUMO is located exclusively on the central thiophene.

3.5. Crystal Structure. The crystallographic properties of BBT, not determined to date, can complement the behavior found by fluorescence. BBT crystallizes in the monoclinic space group $P2_1/n$, with four molecules in the unit cell. The BBT

dx.doi.org/10.1021/jp207136k |J. Phys. Chem. B 2011, 115, 12362–12369

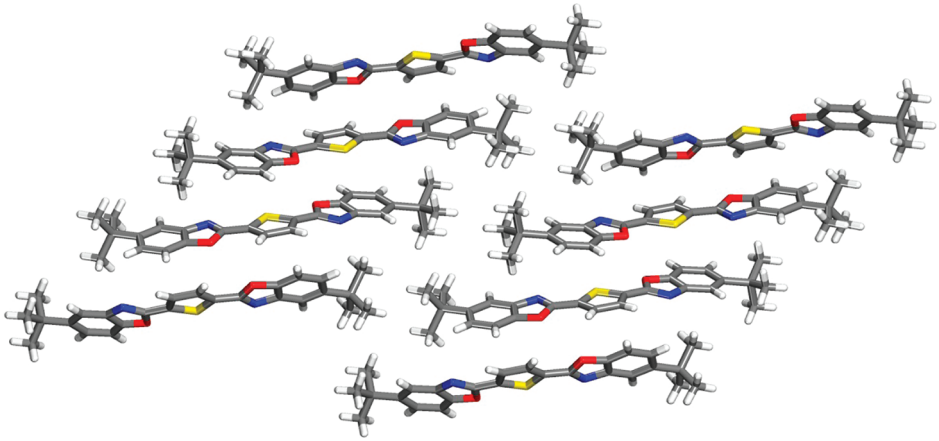

Figure 10. Projection along the *a*-axis showing the BBT crystal packing.

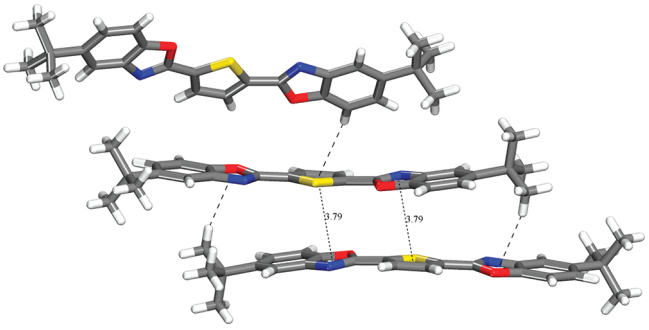

Figure 11. Part of the BBT crystal structure, showing the π-stacking and the C−H···π interaction between two neighboring molecules. For clarity, H atoms bonded to C atoms that are not involved in the motif shown have been omitted. Featured interactions are shown as dashed lines.

molecular structure is characterized by a 2-fold rotation axis passing through the S atom and the midpoint of the C−C single bond in the thiophene ring, but this symmetry is not retained in the crystal phase. According to Figure 9, the two benzoxazolyl rings exhibit a mutual antiorientation, and the whole molecular symmetry is *C*1.

The S1···C2 and S1···C15 bond lengths [1.720 (2) and 1.723 (3) Å] are in good agreement with those found for other structures containing a substituted thiophene ring: 1.709 (2) and 1.709 (2) Å,[33] 1.722 (3) and 1.734 (3) Å,[34] 1.705 (3) and 1.712 (2) Å,[35] 1.726 (17) and 1.727 (18) Å,[36] and 1.707 (6) and 1.729 (6) Å.[37] Moreover, the C2···C3 and C15···C16 bond lengths [1.443 (4) and 1.436 (3) Å] are also comparable to those found in similar molecules [1.460 (2) and 1.455 (2) Å] for the 2,5-bis(1-butyl-benzimidazol-2-yl)thiophene[36] and [1.465 (8) and 1.426 (8) Å] for the 2,5-bis(4-biphenylyl)thiophene.[37]

The dihedral angles between the thiophene plane and benzene rings are 4.95(12)° and 10.43(12)°, and the dihedral angle between these two benzene rings is 11.35(12)°. The benzoxazolyl ring systems are twisted by 4.99(10)° and 10.26(10)° out of the mean plane that passes through the thiophene ring. The whole molecule shows an important deviation from planarity, with the largest deviation from the mean plane of all non-H atoms of −1.7686(26)° for atom C24.The unsymmetrical bow-shaped form of the molecule can be seen in Figure 10. This shape is consistent with the results of a quantum mechanical calculation performed on a simplified model of BBT,[38] leading to a model in which the molecule adopts a complex banana-shaped structure due to the thiophene 2,5-disubstitution that limits the whole molecule planarity.

The dihedral angles between the oxazole and phenyl rings are small: 0.55(12)° and 1.22(13)°. The slight noncoplanarity of the aromatic rings in the solid state[13,39] helps in minimizing intermolecular interactions, thus maintaining the π-orbital overlapping and the conjugation.[40]

The general crystallographic profile is characterized by a layered arrangement with the molecules aligned along the *c*-axis and a low degree of parallelism between them. These banana-shaped molecules exhibit particularly interesting features. The BBT structure is made from a network, alternating layers of molecules showing a limited degree of packing (Figure 10). Within the layers, the molecules pack via moderate $\pi-\pi$ stacking interactions. The π-stacked molecules are staggered relative to each other and overlap at a perpendicular distance of 4.21(1) Å. These interactions involve a distance of 3.79(1) Å between centroids of the five-membered ring of the benzoxazole group and the central thiophene ring. This stacking is limited by the very cumbersome *tert*-butyl groups of two neighboring molecules that come into contact and prevent perfect overlap between the two layers. A similar stacking interaction was observed in 2,5-bis (2-cyano-2-thienylvinyl)thiophene between shifted thiophene rings featuring distances between aryl centroids of 3.78 and 3.91 Å.[41]

The interaction between layers features a C−H···π contact (Figure 11) involving both the thiophene ring and the oxazole ring separated by a distance of 2.82(1) Å between the terminal hydrogen of the *t*-butyl group and the oxazole ring. The distance between the terminal hydrogen of the phenyl ring and the thiophene centroid is 2.81(1) Å. Atoms C9 and C25 in the BBT molecule act as hydrogen-bond donors to the thiophene and oxazole rings of the molecule, respectively (Figure11), independent of the orientation of the aryl acceptors. A similar C−H···π intermolecular interaction was found in 3-(5-chloro-3-methyl-1-phenylpyrazol-4-yl)-1,5-di-2-thienylpentane-1,5-dione.[42] The fluorescence spectrum (Figure 5) corroborates a similar arrangement involving limited and weak C−H···π and $\pi-\pi$-stacking interactions for the aggregates structure, as found in the extended three-dimensional structure of the crystalline material.

4. CONCLUSIONS

BBT is highly fluorescent and might be a suitable replacement for conventional fluorophores such as BBS. Its high fluorescence

yield in most organic solvents, regardless of their polarity and proticity, as well as in polymeric films, further makes BBT a suitable fluorescence reference for actinometric fluorescence studies. BBT is also advantageous because of its photochemical and thermal inertness, in contrast to BBS, which undergoes deformation, temperature, and photoinduced conformational changes. BBT photophysical properties, such as its time-resolved and steady-state behaviors, have been investigated for the first time and reveal that, although the primary deactivation mode of the singlet excited state is by fluorescence, BBT also deactivates by both IC and ISC, albeit collectively <35%. In solution and especially when distributed in semicrystalline PBS, spectral changes and the bathochromic shift shown by BBT as a function of its concentration are due to aggregation of ground state molecules, with the absence of a singlet excited state deactivation by excimer formation confirmed by the monoexponential lifetime of 1.7 ns. The aggregate formation is relatively independent of the BBT concentration, which is in contrast with BBS, which shows concentration-dependent excimer formation. The high fluorescence of BBT, which is solvent-independent, taken together with its high solubility in common organic solvents, makes it a viable sensor for polymeric and solution studies and a potential substitute for the well-known fluorophore BBS, in addition to its probable use as a color indicator. The bent nature of BBT (observed by XRD), which is due to the twisting of the planes of the benzoxazolyl moieties from the plane made by the central thiophene, limits the number of possible intermolecular interactions, making it inherently soluble in most organic solvents. This contrasts with its analogue, BBS, which is soluble only in hot highly boiling chlorinated solvents such as tetrachloroethane.

■ ASSOCIATED CONTENT

Supporting Information. Crystallographic data and steady-state and time-resolved fluorescence spectra. This material is available free of charge via the Internet at http://pubs.acs.org.

■ AUTHOR INFORMATION

Corresponding Author

*E-mail: (W.G.S.) w.skene@umontreal.ca, (R.E.P.) re.prudhomme@umontreal.ca, (C.G.B.) geraldine.bazuin@umontreal.ca.

■ ACKNOWLEDGMENT

The authors gratefully acknowledge financial support from the Canada Foundation for Innovation, Nanoquebec, Centre for Self-Assembled Chemical Structures, Natural Sciences and Engineering Research Council of Canada, and Fonds québecois de la recherche sur la nature et les technologies. W.G.S. thanks the Humboldt Foundation and the Royal Society of Chemistry for fellowships allowing the manuscript to be drafted. A.F. thanks the Tunisian Government for a scholarship of excellence.

■ REFERENCES

(1) Irie, M. *Chem. Rev.* **2000**, *100*, 1685–1716.
(2) Momotake, A.; Arai, T. *J. Photochem. Photobiol. C* **2004**, *5*, 1–25.
(3) Bischoff, P.; Hutter, C.; Puebla, C. E.P. Patent 1,294,846, 2001.
(4) Bur, A. J.; Roth, S. C. *Polym. Eng. Sci.* **2004**, *44*, 898–908.
(5) Pucci, A.; Bertoldo, M.; Bronco, S. *Macromol. Rapid Commun.* **2005**, *26*, 1043–1048.
(6) Pucci, A.; Ruggeri, G.; Bronco, S.; Bertoldo, M.; Cappelli, C.; Ciardelli, F. *Prog. Org. Coat.* **2007**, *58*, 105–116.
(7) Sing, C. E.; Kunzelman, J.; Weder, C. *J. Mater. Chem.* **2009**, *19*, 104–110.
(8) King, N. R.; Whale, E. A.; Davis, F. J.; Gilbert, A.; Mitchell, G. R. *J. Mater. Chem.* **1997**, *7*, 625–630.
(9) Ward, I. M. In *Structure and properties of oriented polymers*; 1st ed.; Applied Science Publishers: London, 1975, pp 1−500.
(10) Liu, M. O.; Lin, H. F.; Yang, M. C.; Lai, M. J.; Chang, C. C.; Liu, H. C.; Shiao, P. L.; Chen, I. M.; Chen, J. Y. *Mater. Lett.* **2006**, *60*, 2132–2137.
(11) Adachi, C.; Tsutsui, T.; Saito, S. *Appl. Phys. Lett.* **1990**, *56*, 799–801.
(12) Kim, J. S.; Seo, B. W.; Han, E. M.; Gu, H. B. *Mol. Cryst. Liq. Cryst.* **2001**, *370*, 35–38.
(13) Kim, J. S.; Seo, B. W.; Gu, H. B. *Synth. Met.* **2003**, *132*, 285–288.
(14) Liu, M.; Guo, B.; Zou, Q.; Du, M.; Jia, D. *Nanotechnology* **2008**, *19*, 205709 (10pp).
(15) Nam, N. P. H.; Cha, S. W.; Kim, B. S.; Choi, D. S.; Jin, J. I. *Synth. Met.* **2002**, *130*, 271–277.
(16) Wang, J.; H., Z.; Mao, H.; Du, Y.; Wang, Y. *J. Lumin.* **2007**, *122-123*, 268–271.
(17) Yamaguchi, R.; Moriyama, K.; Sato, S. *Mol. Cryst. Liq. Cryst.* **2008**, *488*, 210–218.
(18) Yang, J.; Gordon, K. C. *Chem. Phys. Lett.* **2003**, *375*, 649–654.
(19) Yang, J.; Gordon, K. C.; Mc Quillan, A. J.; Zidon, Y.; Shapira, Y. *Phys. Rev. B* 2005, *71*, 155209 (7pp).
(20) Yang, J. H.; Gordon, K.; Robinson, B. H. *Synth. Met.* **2003**, *137*, 999–1000.
(21) Zhang, R.; Z., H.; Shen, J. *Synth. Met.* **1999**, 105.
(22) McGregor, N.; Pardin, C.; Skene, W. G. *Aust. J. Chem.* **2011**, *64*, 10.1071/CH11297.
(23) Kasha, M. *Discuss. Faraday Soc.* **1950**, *9*, 14–19.
(24) Fourati, M. A.; Maris, T.; Bazuin, C. G.; Prud'homme, R. E. *Acta Crystallogr., Sect. C: Cryst. Struct. Commun* **2010**, *66*, o11–o14.
(25) Khun, H.; Braslavsky, S. E.; Schmidt, R. *Pure Appl. Chem* **2004**, *76*, 2105–2146.
(26) Karstens, T.; Kobs, K. *J. Phys. Chem.* **1980**, *84*, 1871–1872.
(27) Bolduc, A.; Dufresne, S.; Hanan, G. S.; Skene, W. G. *Can. J. Chem.* **2010**, *88*, 236–246.
(28) Antoniadis, H.; Inbasekaran, M.; Woo, E. P. *Appl. Phys. Lett.* **1998**, *73*, 3055–3057.
(29) Masetti, F.; Elisei, F.; Mazzucato, U. *J. Lumin.* **1996**, *68*, 15–25.
(30) Lakowicz, J. R. *Principles of Fluorescence Spectroscopy*; 3rd ed.; Springer: New York, 2006.
(31) Grimsdale, A. C.; Leok Chan, K.; Martin, R. E.; Jokisz, P. G.; Holmes, A. B. *Chem. Rev.* **2009**, *109*, 897–1091.
(32) Pope, M.; Swenberg, C. E. In *Electronic Processes in Organic Crystals and Polymers*; 2nd ed.; Oxford University Press: New York, 1999.
(33) Özbey, S.; Kaynak, F. B.; Ertas, E.; Ozturk, T. *Acta Crystallogr., Sect. C: Cryst. Struct. Commun.* **2005**, *61*, o393–o395.
(34) Rodinovskaya, L. A.; Shestopalov, A. M.; Chunikhin, K. S. *Tetrahedron* **2002**, *58*, 4273–4282.
(35) Kazak, C.; Aygün, M.; Turgut, G.; Özbey, S.; Büyükgüngör, O. *Acta Crystallogr., Sect. C: Cryst. Struct. Commun.* **2000**, *56*, 1044–1045.
(36) Pan, W.; Xu, Y.; Sun, Y.; Shao, C.; Lin, D. Y.; Song, H. C. *Analyt. Sci.* **2007**, *23*, x95–x96.
(37) Hotta, S.; Goto, M. *Adv. Mater.* **2002**, *14*, 498–501.
(38) Pucci, A.; Cappelli, C.; Bronco, S.; Ruggeri, G. *J. Phys. Chem. B* **2006**, *110*, 3127–3134.
(39) Ciofalo, M., Ph.D. thesis, University of Pisa, 1992.
(40) Mukamal, S.; Tretiak, S.; Wagersreiter, T.; Chernyak, V. *Science* **1997**, *277*, 781–787.
(41) Wagner, P.; Officer, D. L.; Kubicki, M. *Acta Crystallogr., Sect. E* **2006**, *62*, o5931–o5932.
(42) Trilleras, J.; Quiroga, J.; Cobo, J.; Low, J. N.; Glidewell, C. *Acta Crystallogr., Sect. E* **2005**, *61*, o1892–o1894.